Metallophysics and Advanced Technologies
Металофіз. новітні технол.
Metallofiz. Noveishie Tekhnol.
2022, vol. 44, No. 1, pp. 79–95
https://doi.org/10.15407/mfint.44.01.0079
Reprints available directly from the publisher

PACS numbers: 43.35.+d, 61.46.-w, 68.35.Ct, 68.35.Gy, 81.40.Lm, 81.65.-b

Combination of Laser Shock Peening with Cavitation, Shot and Ultrasonic Impact Hardening for Stainless Steels Surface Characteristics Improving

D. A. Lesyk[*], H. Soyama[**], B. N. Mordyuk[*,***], O. Stamann[****], and V. V. Dzhemelinskyi[*]

[*]*National Technical University of Ukraine 'Igor Sikorsky Kyiv Polytechnic Institute', 37 Peremohy Ave., UA-03056 Kyiv, Ukraine*
[**]*Tohoku University, 6-6-01 Aoba, Aramaki, Aoba-ku, JP-980-8579 Sendai, Japan*
[***]*G. V. Kurdyumov Institute for Metal Physics, N.A.S. of Ukraine, 36 Academician Vernadsky Blvd., UA-03142 Kyiv, Ukraine*
[****]*Otto von Guericke University, 2 Universitätsplatz, DE-39106 Magdeburg, Germany*

This paper's aims are to compare the effects of advanced mechanical surface treatments on the surface characteristics of AISI 304 austenitic stainless steel. The laser shock peening (LSP), combined with the water jet cavitation peening (WjCP), water jet shot peening (WjSP), and multi-pin ultrasonic impact peening (UIP), is applied to improve the surface quality and increase the hardness, hardening depth, and the compressive residual stress values in the near-surface layers. The laser shock processing is implemented using a submerged laser peening system with a wavelength of 1064 nm. The outcomes of the LSP treatment combined with other peening techniques in different sequences (applied prior or post it) are studied. The experimental results show as compared to the combined LSP + WjCP and LSP + WjSP techniques, the

Corresponding author: Dmytro Anatoliyovych Lesyk
E-mail: lesyk_d@ukr.net

Citation: D. A. Lesyk, H. Soyama, B. N. Mordyuk, O. Stamann, and V. V. Dzhemelinskyi, Combination of Laser Shock Peening with Cavitation, Shot and Ultrasonic Impact Hardening for Stainless Steels Surface Characteristics Improving, *Metallofiz. Noveishie Tekhnol.*, **44**, No. 1: 79–95 (2021). DOI: 10.15407/mfint.44.01.0079

combined LSP + UIP technique results in a lower surface roughness ($Ra \sim 0.15$ μm) and higher surface macrohardness (~ 39.0 HRC_5) supported by nanoscale grain structure with grain size of 15–100 nm, which is observed by XRD and TEM analysis. The surface macrohardness is respectively increased by about 48%, 68%, and 80% after the combined WjCP + LSP, WjSP + LSP, and UIP + LSP techniques in comparison with the original sample (22.1 HRC_5). All combined peening techniques lead to an increase in the residual stresses values as compared to the single LSP process, providing the hardening depth of about 1 mm.

Key words: AISI 304 stainless steel, laser shock peening, water jet cavitation/shot peening, ultrasonic impact peening, roughness, hardness, nanostructure.

Метою даної роботи є порівняння впливу передових методів механічної поверхневої обробки на характеристики поверхні аустенітної неіржавкої сталі 08Х18Н10. Лазерне ударне зміцнення (LSP) у поєднанні з гідроструменевим зміцненням у воді (WjCP), дробоструменевим зміцненням у воді (WjSP) та ультразвуковим ударним зміцненням багатобойковим наконечником (UIP) застосовують для поліпшення якості поверхні і збільшення величин твердості, глибини зміцнення та залишкових напружень стискання у приповерхневих шарах. Лазерну ударну обробку здійснено за допомогою зануреної системи лазерного зміцнення з довжиною хвилі 1064 нм. Досліджували результати лазерного ударного зміцнення у поєднанні з іншими методами зміцнення у різних послідовностях (застосовували до або після нього). Експериментальні результати показали, що порівняно з комбінованими методами LSP + WjCP та LSP + WjSP, комбінований метод LSP + UIP призводить до меншої шорсткості поверхні ($Ra \sim 0{,}15$ мкм) та вищої поверхневої макротвердості (~ 39,0 HRC_5), що підтверджує нанорозмірну зеренну структуру з розміром зерен 15–100 нм, яка спостерігалася за допомогою рентґеноструктурного аналізу та трансмісійної електронної мікроскопії. Поверхнева макротвердість збільшується приблизно на 48, 68 та 80%, відповідно, після комбінованих методів WjCP + LSP, WjSP + LSP та UIP + LSP порівняно з вихідним зразком (22,1 HRC_5). Усі комбіновані методи зміцнення призводять до збільшення значень залишкових напружень порівняно з одиничним процесом LSP, забезпечуючи глибину зміцнення приблизно 1 мм.

Ключові слова: неіржавка сталь 08Х18Н10, лазерне ударне зміцнення, гідроструменеве/дробоструменеве зміцнення у воді, ультразвукове ударне зміцнення, шорсткість, твердість, наноструктура.

(Received October 22, 2021)

1. INTRODUCTION

Given the high technological requirements for industrial products, special attention is paid to their reliability and durability. As well-known that the metal surface of components is exposed to intense me-

chanical, thermal, chemical, and other influences. Thus, the main cause of premature failure of parts is the destruction and wear of the surface layer.

Currently, both traditional and advanced highly concentrated surface treatment methods are used to form the required material properties for the fatigue and corrosion/wear resistance of metal components. One of the most effective solutions is the application of the laser surface modification techniques in combination with advanced mechanical surface treatments to enhance the surface characteristics [1–3]. The combination of individual types of modification techniques allows obtaining a much greater effect in increasing the surface characteristics of metal parts to prolong their operation life.

There are several laser surface modification methods, such as a laser shock peening [4, 5], laser transformation hardening [6], laser surface melting/alloying [1, 2], and laser surface cladding [7]. It is also important to point out that the laser shock peening or laser transformation hardening techniques can improve the surface properties, retaining the same chemical composition of the material. Recently, the laser transformation hardening combined with the ultrasonic impact hardening is applied to reduce the surface roughness and increase the surface hardness, forming the compressive residual stresses in carbon [8] and tool [9] steels. The laser transformation hardening is effective for surface treatment of structural or tool steels with a high carbon content of more than 0.3% in which an ultrafine martensitic microstructure in the subsurface layer is formed due to phase transformations.

However, to improve the surface characteristics in low carbon steels, the surface plastic deformation methods, such as a shot blasting (SB) [10], shot peening (SP) [11], water jet shot peening (WjSP) [12], cavitation peening (CP) [13], water jet cavitation peening (WjCP) [14], ultrasonic impact peening [15–17], ultrasonic burnishing (USB) [10, 18], and laser shock peening (LSP) [19–21] are usually applied. All of the above-mentioned mechanical surface treatments can be used for surface peening of the complex-shape or large-sized parts. In comparison with the unprocessed rough specimen, the surface roughness is slightly decreased after the LSP and WjCP processes, while the WjSP and multi-pin UIP processes lead to a significant reduction of the parameter *Ra* due to the plastic deformation both peaks and valley of initial micro-irregularities [22]. Conversely, the LSP and WjCP processes provided a greater hardening depth thanks to a higher strain rate as compared to the WjSP and UIP processes. The surface nanocrystallization process of stainless steels is reported elsewhere [23–26].

Additionally, a study of stainless steel by Turski *et al.* [20] established that as compared to the conventional SP process, the LSP, monopin UIP, and WjCP processes induced a greater depth of compressive residual stress.

However, it is of interest that the combined peening techniques provide a better improvement of the surface characteristics as compared to the single peening process [27–30]. Wang *et al.* [31] found favourable effects of the application of LSP followed by SP for surface enhancement of a martensitic stainless steel. Unal *et al.* [30] studied the effects of SB combined with SP on the surface roughness, hardness, and structure of the AISI 304 stainless steel. They have shown that the surface roughness is decreased after the SP process followed by the SB process. Soyama *et al.* [27] established that a combination of WjCP + CP/CP + WjCP, SP + WjCP/WjCP + SP, and CP + SP/SP + CP induced the resistance to fatigue crack growth owning to a greater and deeper compressive residual stress in comparison with a single peening of AISI 316L austenitic stainless steel. Zhang *et al.* [32] showed that the combined USB + SP + USB process increased the surface hardness value from ~ 800 $HV_{0.2}$ to ~ 1100 $HV_{0.2}$ and value of the surface compressive residual stress from about –350 MPa to –1000 MPa. Kumar *et al.* [29] recommended the SP followed by deep cold rolling (DCR) to increase the fatigue life.

Based on the chemical, thermal, and mechanical influence, the thermo-mechanical surface treatment [1, 2, 9, 33] or thermochemical treatment combined with the mechanical surface treatment [34–36] can also be applied to enhance the fatigue life and corrosion/wear resistance of the treated surface by generation of a hard layer. Shen *et al.* [34] revealed that a pre-shot peening allows a double increase in the thicker nitrided layer as compared to the unpeened surface by increasing the nitrogen diffusion rate of stainless steel. The effects of the SP, USB, and DCR techniques on the plasma-carburized surface are studied in works [37–39].

It should also be noted that among peening techniques, the LSP technique is one of the most effective techniques for selective surface treatment of fatigue-prone metals that produces a deep hardening depth and compressive residual stress in the near-surface layers [40]. The surface of a metal part is impacted by a pulsed laser beam to generate high-energy plasma, which produces a pressure wave. The LSP technique leads to significantly deeper compressive residual stresses than conventional peening techniques, providing a superior surface enhancement for the resistance of materials to fatigue and stress corrosion cracking [41]. Nevertheless, despite successful LSP examples for surface treatment of metal parts (turbine blades and compressors, car engine parts, aircraft wings, parts of rockets and satellites, gears and shafts of propeller gears, *etc.*), this method suffers from a poor surface quality and inhomogeneous properties of the hardened layer.

Thus, to improve both the surface quality and material properties in the low carbon steels or stainless steels treated by the LSP technique, post-processing is required. As a consequence, the development of new

combined pre- or post-processing techniques for expanding opportunities of LSP technique for advanced manufacturing is very relevant.

The paper compares the effects of the WjCP, WjSP, and multi-pin ultrasonic impact peening (UIP) processes on the surface roughness, hardness, and residual stresses of the austenitic stainless steel AISI 304 treated by LSP. The study of the combined WjCP + LSP, WjSP + LSP, and UIP + LSP techniques is also addressed.

2. EXPERIMENTAL DETAILS

The plane samples with a dimension of 48×48×3 mm^3 of AISI 304 austenitic stainless steel in as-received condition are applied. The unpolished samples are rough ($Ra = 3.063$ μm). The chemical composition of studied steel is ~18% Cr, ~9% Ni, ~0.8% Si, ~0.5% Ti, 0.3% Cu, 0.2% Mn, 0.08% C, and balance Fe. The cross-section microhardness near the surface is 230 $HV_{0.1}$, while the surface hardness is 22.1 HRC_5. The samples are processed by a laser peening, cavitation peening, shot

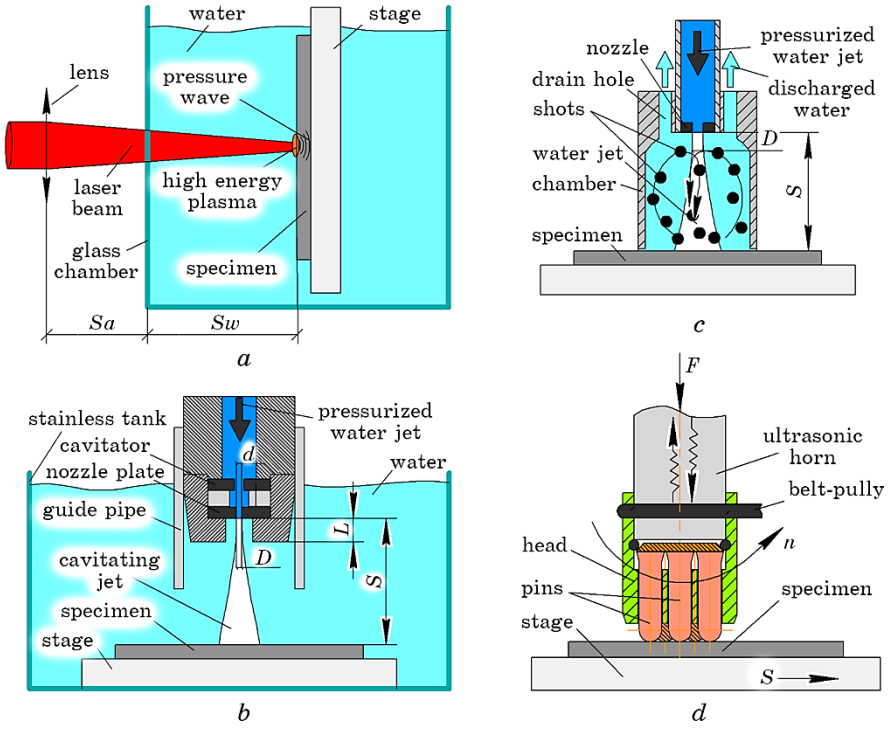

Fig. 1. Schematic representation of the experimental setups applied for the laser shock peening (*a*), water jet cavitation peening (*b*), water jet shot peening (*c*), and multi-pin ultrasonic impact peening (*d*).

peening, and ultrasonic peening with the optimized parameters [22].

The laser shock peening (LSP) process is implemented using a Nd:YAG laser with the wavelength of 1.06 μm [42]. Figure 1, *a* reveals the setup for the submerged LSP technique. The sample is placed on a stage that moved horizontally and vertically by stepping motors in a water-filled glass chamber. The laser beam is focused on the treated sample using a plano-convex lens, providing the laser spot size of 0.8 mm on the treated surface. The LSP experiments are made at a pulse energy of 0.35 J and a pulse width of 6 ns. During the LSP process, the laser beam is overlapped by 50% . The pulse number density is 8 pulses/mm^2.

The cavitation peeing (WjCP) process using a submerged water jet is realized into a water-filled stainless-steel tank (Fig. 1, *b*). The pressurized water jet by a plunger pump is perpendicularly injected into the treated surface. A detailed description of the WjCP system can be found elsewhere [22, 42, 43]. The WjCP technique is carried out by a jet injection pressure of 30 MPa and a jet ambient pressure of 0.1 MPa. The nozzle throat diameter D is 2 mm, the diameter of the cavitator d is 3 mm, and the stand-off distance S between the nozzle and the surface sample is 222 mm. The treatment time is 8 s/mm providing a peened patch size of 45×45 mm^2.

The shot peening (WjSP) process is performed applying recirculating shots accelerated by a pressurized water jet which come through three 0.8 mm diameter holes [42]. A peening head for WjSP technique is given in Fig. 1, *c*. The WjSP tests are conducted in the chamber with an inner diameter of 54 mm at a water-jet an injection pressure of 12 MPa using 500 stainless steel shots/balls in a diameter of 3.2 mm. The stand-off distance S from the nozzle to the sample surface is 50 mm (Fig. 1, *c*). During the WjSP process, the samples are uniformly peened by moving the chamber at constant speed [44]. The WjSP duration is 0.88 s/mm while a peened area is 45×45 mm^2.

UIP process is performed by a numerical control milling machine, a 0.3 kW ultrasonic generator, and a multi-pin ultrasonic impact tool. An ultrasonic vibration system is attached to a conventional machine-tool (Dyna Myte 2800) with numerical control and passed to the specimen surface at a static load of 50 N. A seven-pin impact head is mounted at a step-like waveguide horn tip. Fig. 1, *d* illustrates a schematic diagram of the multi-pin impact head. The multi-pin UIP system is described in detail [3, 22, 23]. The UIP experiments are carried out at a vibration frequency f_{UIP} of 21.6 kHz and amplitude AUIP of ultrasonic horn tip of 15 μm. During the UIP process, the multi-pin impact head is forcedly rotated by a motor at a rotation speed of 76 rpm. The UIP process lasted for 60 s.

The surface texture of the samples in an area of 4.5×5 mm^2 is measured using a 3*D* optical surface system (Leica DCM 3*D*). The surface

roughness parameters of all samples are estimated using a filter cut-off of 0.8 mm in each measurement. The profile arithmetic mean parameter *Ra* is defined six times at different places and the roughness of each state is averaged.

The surface macrohardness is measured using a universal digital hardness tester (Computest SC) at a load on indenter of 49 N. In each case, six measurements are conducted in different locations of the peened zones and average value summarized. The microhardness depth measurements in the near-surface layer are performed at the loads of 0.1 kg ($HV_{0.1}$) and 0.025 kg ($HV_{0.025}$) using a PMT-3 microhardness tester.

Microstructure of the surface layers is analysed by transmission electron microscopy (a JEM 100 CX-II microscope) and X-ray diffraction (XRD) structural-phase analysis using a Rigaku Ultima IV diffractometer (CuK_α) in 'θ–2θ' geometry with a 2θ (20–120°) scanning speed of 2°/min. The residual stress measurements are performed using sin2ψ based method [44]. The diffraction angle from the γ-Fe (220) plane without strain is 128 degrees. To calculate the stress tensor, the diffraction ring from the sample is detected at several angles (φ and ψ).

3. RESULTS AND DISCUSSION

3.1. Surface Morphology

The surface morphology of the samples recorded with the laser profilometer is illustrated in Fig. 2 while surface roughness parameter *Ra*

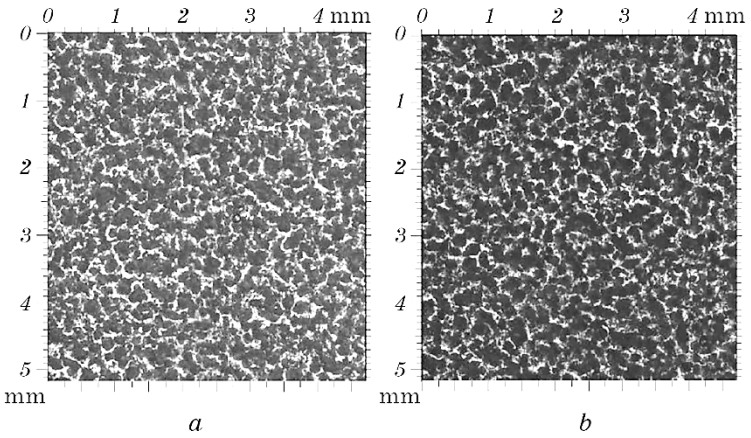

Fig. 2. Comparison of 2*D* surface morphology of the unpeened sample (*a*) and after LSP (*b*), combined LSP + WjCP (*c*), WjCP + LSP (*d*), LSP + WjSP (*e*), WjSP + LSP (*f*), LSP + UIP (*g*), and UIP + LSP (*h*) peened AISI 304 samples.

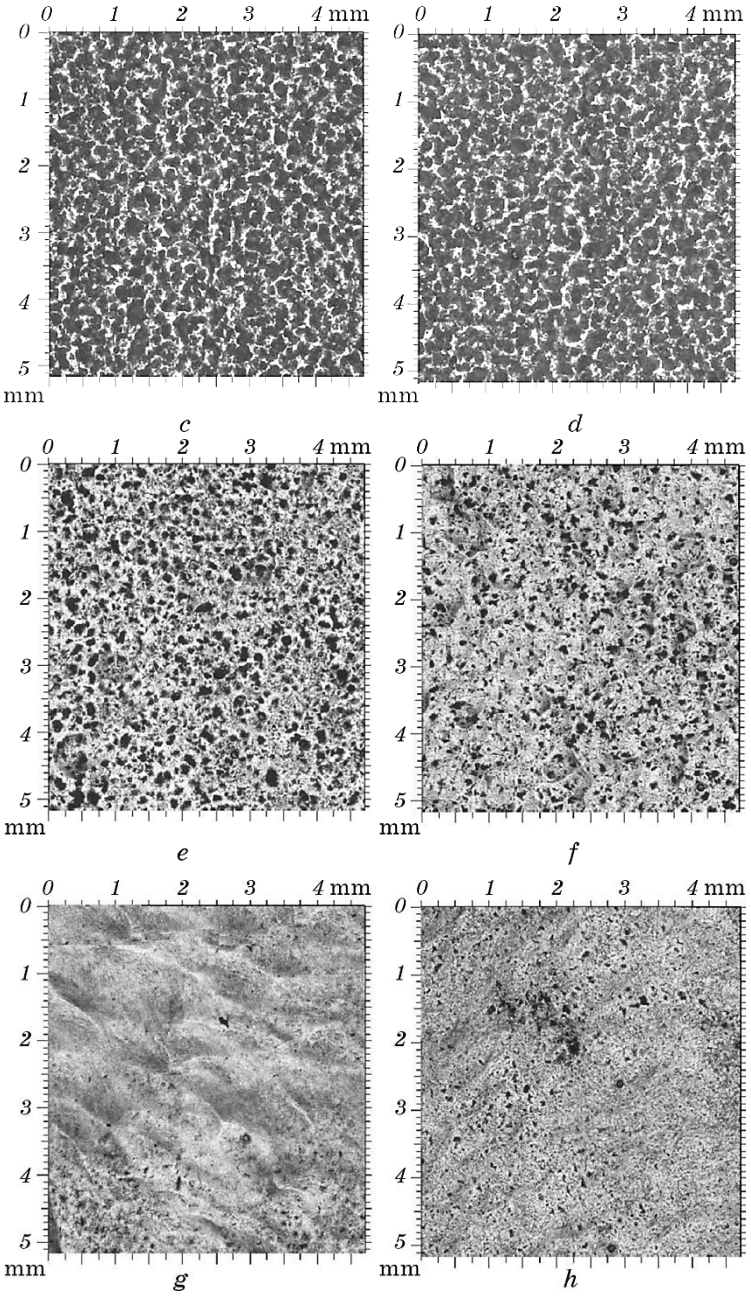

Continuation of Fig. 2.

is presented in Fig. 3.

It is of interest that in comparison with the unpeened sample (Fig. 2,

a), the surface texture in the LSP-peened and combined LSP + WjCP and WjCP + LSP-peened samples are slightly changed due to rather rough initial surface (surface maximum height parameter $Sz \sim 39$ μm). The same results are observed in work [21]. Nevertheless, it is well-known that the LSP technique leads to an increase in the roughness and waviness parameters due to the surface severe plastic deformation by highly concentrated laser shots [19]. The effects of LSP and WjCP techniques on the surface texture of studied steel are presented in our recent work [22].

The parameter *Ra* is slightly decreased by the combined LSP + WjCP and WjCP + LSP techniques in comparison with the single LSP and WjCP-peened sample (Fig. 3). Compared to the initial state, the combination of LSP and WjSP processes allows almost double increasing the surface roughness, forming a new wavy surface texture/microrelief (Fig. 2). At the same time, the surface maximum profile height of the combined WjSP + LSP-processed samples ($Sz \sim 28$ μm) is lower than that of the combined LSP + WjSP-processed samples ($Sz \sim 43$ μm).

The surface roughness is remarkably decreased after the application of UIP both pre-LSP ($Ra \sim 0.35$ μm) and post-LSP ($Ra \sim 0.15$ μm) (Fig. 3). This is because of the rotated multi-pin head which provides the sliding impact of seven pins by the sample surface. This result also correlates well with the literature data [3, 8]. Moreover, as compared to the combined LSP + WjCP and LSP + WjSP techniques, the combined LSP + UIP technique forms a regular microrelief with lower roughness parameters due to the application of the multi-pin ultrason-

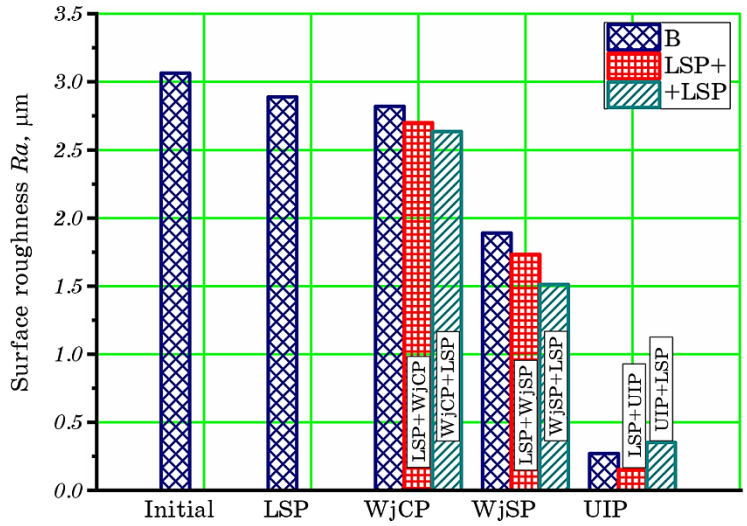

Fig. 3. Comparison of surface roughness *Ra* magnitudes of the unpeened sample and after LSP, WjCP, WjSP, UIP, and combined peened AISI 304 samples.

ic tool which moved by a Computer Numerical Control (CNC) program and rotated forcedly by a motor. It should also be noted that the LSP process increased the surface roughness in the UIP-processed sample. As compared to the initial state, the parameter *Ra* is respectively reduced by approximately 13%, 80%, and more than triple after combined LSP + WjCP, LSP + WjSP, and LSP + UIP methods. In contrast to the combined UIP + LSP technique, the parameter *Ra* is decreased after the combined WjCP + LSP and WjCP + LSP techniques as well.

3.2. Surface Hardness

The experiments show that the surface macrohardness (HRC_5) increases relative to the single peened samples irrespective of the combined peening type (Fig. 4).

The highest surface hardness is observed after the combined LSP + UIP/UIP + LSP and LSP + WjSP/WjSP + LSP techniques (~ 38 HRC_5), and the lower surface hardness is conversely observed after the combined LSP + WjCP/WjCP + LSP methods (~ 32 $HV_{0.1}$). The figures point to the surface severe plastic strain with post-LSP leads to a higher surface hardness improvement except for the WjSP + LSP process. In comparison with the unpeened sample (22.1 HRC_5) the surface hardness is increased by about 48, 68, and 80% after the combined WjCP + LSP, WjSP + LSP, and UIP + LSP techniques, respectively.

A near-surface microhardness depth profiles are presented in Fig. 5.

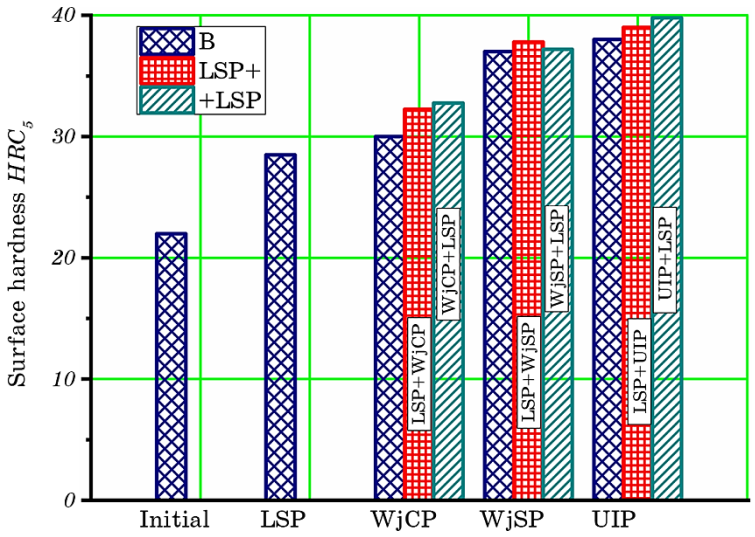

Fig. 4. Comparison of surface hardness HRC_5 magnitudes of the unpeened sample and after LSP, WjCP, WjSP, UIP, and combined peened AISI 304 samples.

The subsurface microhardness of the unpeened sample (~ 230 $HV_{0.1}$) is enlarged after the application of all combined hardening methods, producing the hardened layers of ~ 1 mm thick. This is because the combined peening techniques induced a higher plastic strain in the near-surface increasing grain refinement and dislocation density [15, 25, 29, 30]. The highest values of the surface microhardness are observed after the combined LSP + WjSP (~ 410 $HV_{0.025}$), LSP + UIP (~ 450 $HV_{0.025}$) (Fig. 5, *a*) and UIP/WjSP + LSP (~ 460 $HV_{0.025}$) methods (Fig. 5, *b*) with one exception of combined LSP + WjCP method that shows slightly higher surface microhardness (~ 450 $HV_{0.025}$) in the surface layer (Fig. 5, *a*).

3.3. Microstructure and Residual Stress

X-ray diffraction analysis of the modified surface layers demonstrates that in comparison with the initial specimen all peaks related to austenite f.c.c. phase became shifted to lower diffraction angles indicating the formation of residual compressive stresses. Figure 6 compares residual stresses in the near-surface layers measured by sin2ψ based method. Unlike the LSP followed by the WjCP, WjSP or UIP processes, the prior plastic deformation with post-LSP leads to higher values of

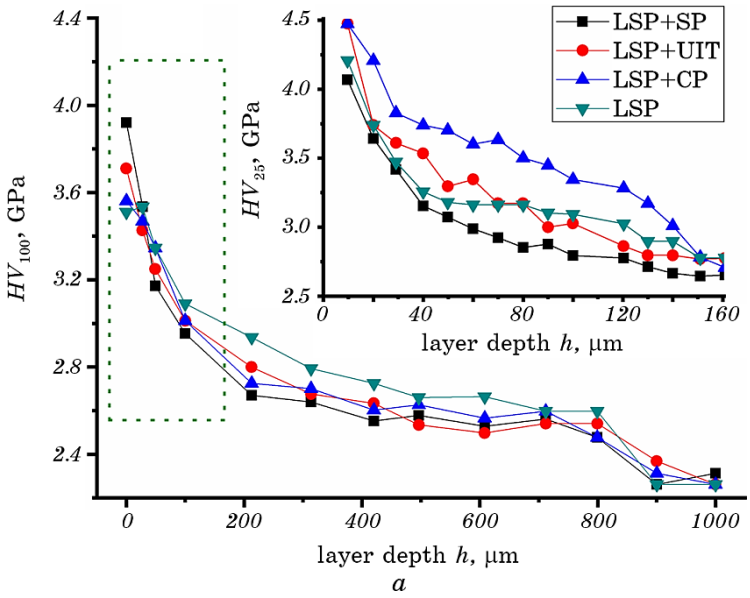

Fig. 5. Microhardness depth profiles $HV_{0.025}$ and $HV_{0.1}$ of LSP and combined LSP + WjCP/WjSP/UIP (*a*) and WjCP/WjSP/UIP + LSP (*b*) peened AISI 304 samples.

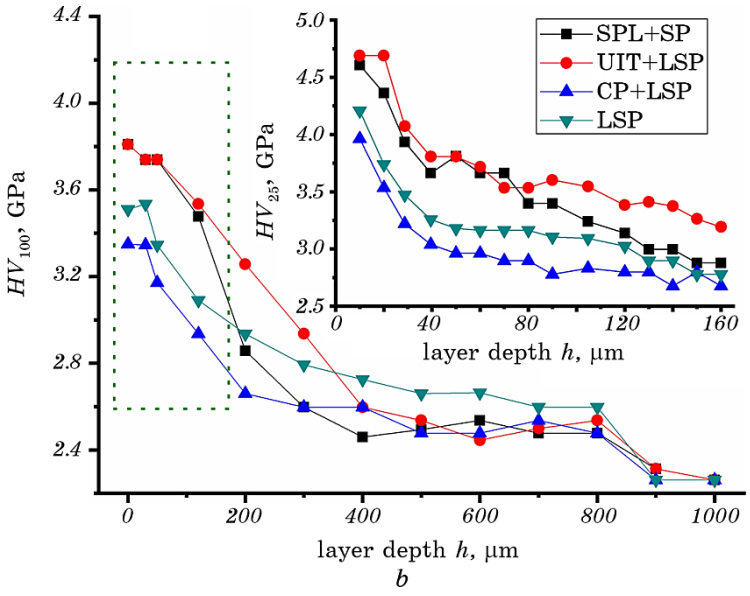

Continuation of Fig. 5.

surface residual stress.

The LSP process combined with the WjCP process increased surface residual stress is –(500–540) MPa as compared to both single LSP (–470 MPa) and WjCP (–377 MPa) techniques, however, the values of

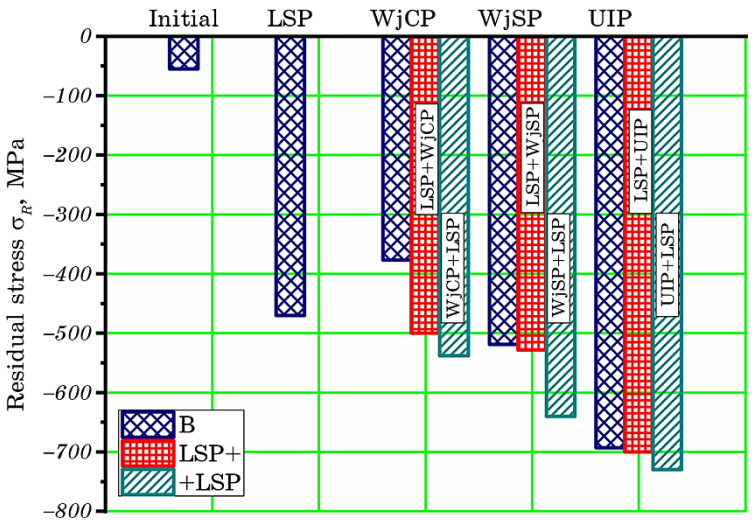

Fig. 6. Comparison of residual stress magnitudes in the unpeened sample and after LSP, WjCP, WjSP, UIP, and combined peened AISI 304 samples.

the residual stress in comparison with the combined LSP + WjSP/UIP and WjSP/UIP + LSP techniques are lower.

The maximum residual stress values are about –640 MPa after the combined WjSP + LSP method, while the combined UIP + LSP method leads to greater residual stress values is –730 MPa.

The change in the residual stress values correlates well with the surface macrohardness data (Fig. 4). The comparison between the effects of cavitation peening in air/water and WjSP processes on the residual stress profile in the subsurface layer of AISI 316 austenitic stainless is studied in works [27, 44]. Results showed that in comparison with a single peening process, the values of the compressive residual stresses are greater and deeper in the samples peened by the combined peening techniques.

Additionally, XRD analyses show that all mechanical treatments used resulted in the appearance of additional peaks related to the martensitic b.c.t. phase. Figure 7 demonstrates fragments of X-ray spectra for the untreated AISI 304 sample containing XRD peaks of only f.c.c. austenite and for the samples modified by LSP and its combination with UIP treatment. The LSP and LSP + UIP combined processes demonstrated the highest magnitudes of the surface macrohardness HRC_5 (Fig. 4) and compressive residual stresses (Fig. 6). It is seen that both austenite and martensite related peaks on the XRD patterns of the modified surfaces are significantly broadened indicating the

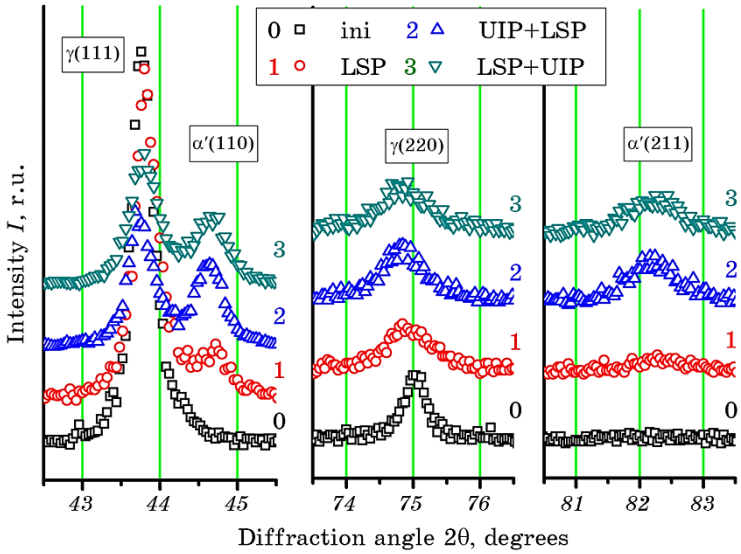

Fig. 7. Fragments of X-ray spectra for the untreated sample and after LSP, and combined UIP + LSP and LSP + UIP peened AISI 304 samples.

grains/crystallites' refinement and/or increased lattice microstrains formed. However, considering the intensity of martensitic peaks, the LSP treatment results in a much lesser volume fraction of α' phase.

A significant decrease in the crystallites size is confirmed by direct observations of the microstructure of near-surface layers of the modified samples by TEM analysis (Fig. 8). For the sake of comparison, microstructures of the LSP treated (Fig. 8, *a*, *b*) and LSP + UIP treated (Fig. 8, *c*, *d*) are presented. The microstructure of the LSP treated surface layer of AISI 304 steel mainly contains dislocation cells with highly tangled boundaries and cell sizes of 150–500 nm. Considering significant azimuthal dispersion of diffraction spots some of the cells are highly misoriented. This well correlated to the data reported to the LSP treated austenitic steel AISI 321 [15]. This microstructure undergoes further refinement during additional UIP treatment. High-density dislocations formation and movement lead to the increase in the volume fraction of the high-angle boundaries transforming dislocation cells into highly misoriented grains. As a result, a nanoscale grain structure with grain size of the 15–100 nm is formed after LSP + UIP treatment (Fig. 8, *c*, *d*). A characteristic ring-like SAED pattern is registered for this nanoscale structure. Similar nanostructurization is reported for UIP treated austenitic steel AISI 321 [15, 45]. Such nanograined structure is believed to be the main reason for the highest observed magnitude of macrohardness HRC_5 (Fig. 4).

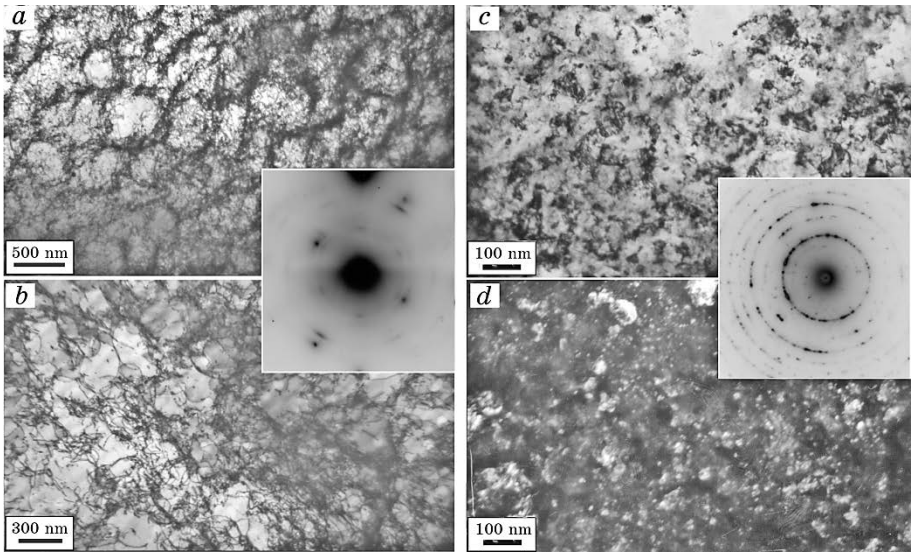

Fig. 8. Bright-field (*a*–*c*) and dark-field (*d*) TEM images of microstructure of AISI 304 samples after LSP (*a*, *b*) and LSP + UIP (*c*, *d*) accompanied with SAED patterns.

4. CONCLUSION

In this paper, AISI 304 stainless steel are peened by LSP and combined peening techniques by a prequential or subsequent LSP treatment (LSP + WjCP/WjCP + LSP, LSP + WjSP/WjSP + LSP, LSP + UIP/UIP + + LSP). The comparison of the surface texture, roughness, hardness, hardening depth, and stress state of AISI 304 stainless steel are estimated. The obtained results allow drawing the following conclusions:

1. The LSP combined with the UIP technique remarkably decreased the mean roughness (parameter *Ra*) of peened surfaces (*Ra* ~ 0.2 μm). Unlike the combined LSP + WjCP and WjCP + LSP techniques, the LSP combined with the WjSP and UIP techniques produce a new surface relief.
2. The surface plastic deformation with post-LSP leads to a higher surface hardness and residual stress improvement as compared to pre-LSP. In particular, the maximum surface hardness is approx. 39 HRC_5 after the combined UIP + LSP/UIP + LSP techniques while the LSP combined with the WjSP (~ 37 HRC_5) and WjCP (~ 32 HRC_5) techniques leads to lower surface hardness. All combined surface peening techniques induced the hardening depth of approx. 1 mm.
3. The maximum surface residual stress is approximation −540 MPa and −640 MPa after the combined WjCP + LSP and WjSP + LSP techniques, respectively, while the combined UIP + LSP technique leads to a higher residual stress (−730 MPa).
4. Mechanical surface treatments result in significant grains/subgrains refinement. Ultrafine dislocation cell structure with cell size of 150–500 nm and highly misoriented nanoscale grain structure with grain size of 15–100 nm are respectively observed in the top near-surface layers of the LSP and LSP + UIP treated samples.
5. The combined LSP + UIP technique can be applied to improve both surface quality and physical and mechanical properties while combined WjCP/WjSP + LSP techniques can be recommended when a higher surface roughness parameters are required.
6. To treat the complexly-shaped or small-sized metal components the application of the LSP and multi-pin UIP methods should be applied for surface peening of the large-sized metal components.

This study is partially supported by JSPS KAKENHI Grant Number 17H03138 and the German Academic Exchange Service (DAAD) Research Grant.

The authors gratefully acknowledge Dr. S. Martinez (Aeronautics Advanced Manufacturing Centre of the University of the Basque Country, Bilbao, Spain) for the support provided with the surface morphology analysis.

REFERENCES

1. Y. Morisada, H. Fujii, T. Mizuno, G. Abe, T. Nagaoka, and M. Fukusumi, *Mater. Sci. Eng. A*, **505**: 157 (2009).
2. J. Radziejewska, *Mater. Des.*, **32**: 5073 (2011).
3. D. A. Lesyk, S. Martinez, V. V. Dzhemelinskyy, A. Lamikiz, B. N. Mordyuk, and G. I. Prokopenko, *Surf. Coat. Technol.*, **278**: 108 (2015).
4. R. Sundar, P. Ganesh, R. K. Gupta, G. Ragvendra, B. K. Pant, V. Kain, K. Ranganathan, R. Kaul, and K. S. Bindra, *Lasers Manuf. Mater. Process.*, **6**: 424 (2019).
5. L. Petan, J. Grum, J. A. Porro, J. L. Ocana, and R. Sturm, *Metals*, **9**: 1271 (2019).
6. S. Martinez, A. Lamikiz, E. Ukar, I. Tabernero, and I. Arrizubieta, *Appl. Therm. Eng.*, **98**: 49 (2016).
7. M. A. Montealegre, G. Castro, P. Rey, J. L. Arias, P. Vazquez, and M. Gonzalez, *Contemp. Mater.*, **19**: 19 (2010).
8. D. A. Lesyk, S. Martinez, B. N. Mordyuk, V. V. Dzhemelinskyi, A. Lamikiz, and G. I. Prokopenko, *Opt. Laser Technol.*, **111**: 424 (2019).
9. D. A. Lesyk, S. Martinez, B. N. Mordyuk, V. V. Dzhemelinskyi, A. Lamikiz, G. I. Prokopenko, Yu. V. Milman, and K. E. Grinkevych, *Surf. Coat. Technol.*, **328**: 344 (2017).
10. Y. He, K. Li, I. S. Cho, C. S. Lee, I. G. Park, J.-i. Song, C.-W. Yang, J.-H. Lee, and K. Shin, *Appl. Microsc.*, **45**: 155 (2015).
11. M. Chaib, M. Belhamiani, A. Megueni, A. Ziadi, and F. J. Belzunce, *Int. J. Mater. Process. Techol.*, **53**: 298 (2016).
12. X. Wei, D. Zhu, X. Ling, L. Yu, and M. Dai, *Int. J. Electrochem. Sci.*, **13**: 4198 (2018).
13. A. Azhari, C. Schindler, E. Kerscher, and P. Grad, *Int. J. Adv. Manuf. Technol.*, **63**: 1035 (2012).
14. H. Soyama, *Int. J. Peen. Sci. Technol.*, **1**: 3 (2017).
15. B. N. Mordyuk, Yu. V. Milman, M. O. Iefimov, G. I. Prokopenko, V. V. Silberschmidt, M. I. Danylenko, and A. V. Kotko, *Surf. Coat. Technol.*, **202**: 4875 (2008).
16. L. Li, M. Kim, S. Lee, M. Bae, and D. Lee, *Surf. Coat. Technol.*, **307**: 517 (2016).
17. X. Yang, X. Wang, X. Ling, and D. Wang, *Results. Phys.*, **7**: 1412 (2017).
18. M. Yasuoka, P. Wang, K. Zhang, Z. Qiu, K. Kusaka, Y. S. Pyoun, and R. Murakami, *Surf. Coat. Technol.*, **218**: 93 (2013).
19. A. Gill, A. Telang, S. R. Mannava, D. Qian, Y. S. Pyoun, H. Soyama, and V. K. Vasudevan, *Mater. Sci. Eng. A*, **576**: 346 (2013).
20. M. Turski, S. Clitheroe, A. D. Evans, C. Rodopoulos, D. J. Hughes, and P. J. Withers, *Appl. Phys. A*, **99**: 549 (2010).
21. J. Epp and H. W. Zoch, *J. Heat Treat. Mater.*, **71**: 109 (2016).
22. D. A. Lesyk, H. Soyama, B. N. Mordyuk, V. V. Dzhemelinskyi, S. Martinez, N. I. Khripta, and A. Lamikiz, *J. Mater. Eng. Perform.*, **28**: 5307 (2019).
23. D. A. Lesyk, B. N. Mordyuk, V. V. Dzhemelinskyi, G. I. Prokopenko, and O. O. Danyleiko, *Sci. Rev.*, **2**: 3 (2018).
24. P. Tadge, P. K. Gupta, and C. Sasikumar, *Mater. Today: Proc.*, **2**: 3245 (2015).
25. M. O. Vasylyev, B. M. Mordyuk, S. I. Sydorenko, S. M. Voloshko, A. P. Burmak, and N. V. Franchik, *Metallofiz. Noveishie Tekhnol.*, **39**, No. 7:

905 (2017) (in Ukrainian).
26. M. A. Vasylyev, B. N. Mordyuk, S. I. Sidorenko, S. M. Voloshko, and A. P. Burmak, *Surf. Coat. Technol.*, **343**: 57 (2018).
27. O. Takakuwa, K. Yamamiya, and H. Soyama, *J. Solid Mechanics Mater. Eng.*, **7**: 357 (2013).
28. Q. Feng, J. She, X. Wu, C. Wang, and C. Jiang, *J. Mater. Eng. Perform.*, **27**: 1396 (2018).
29. D. Kumar, S. Idapalapati, W. Wang, and S. Narasimalu, *Mater.*, **12**: 2503 (2019).
30. O. Unal and R. Varol, *Appl. Surf. Sci.*, **351**: 289 (2015).
31. Z. Wang, C. Jiang, X. Gan, Y. Chen, and V. Ji, *Int. J. Fatigue*, **33**: 549 (2011).
32. Y. Zhang, S. Qu, F. Lu, F. Lai, V. Ji, H. Liu, and X. Li, *Int. J. Fatigue*, **141**: 105867 (2020).
33. D. A. Lesyk, B. N. Mordyuk, S. Martinez, M. O. Iefimov, V. V. Dzhemelinskyi, and A. Lamikiz, *Surf. Coat. Technol.*, **401**: 126275 (2020).
34. L. Shen, L. Wang, Y. Wang, and C. Wang, *Surf. Coat. Technol.*, **214**: 3222 (2010).
35. M. Chemkhi, D. Retraint, A. Roos, C. Garnier, L. Waltz, C. Demangel, and G. Proust, *Surf. Coat. Technol.*, **221**: 191 (2013).
36. A. Toppo, R. Kaul, M. G. Pujar, U. K. Mudali, and L. M. Kukreja, *J. Mater. Eng. Perform.*, **22**: 632 (2013).
37. N. Tsuji, S. Tanaka, and T. Takasugi, *Surf. Coat. Technol.*, **203**: 1400 (2009).
38. N. Tsuji, S. Tanaka, and T. Takasugi, *Mater. Sci. Eng. A*, **499**: 482 (2008).
39. B. Wu, P. Wang, Y.-S. Pyoun, J. Zhang, and R.-I. Murakami, *Surf. Coat. Technol.*, **213**: 271 (2012).
40. S. Prabhakaran, A. Kulkarni, G. Vasanth, S. Kalainathan, P. Shukla, and V. K. Vasudevan, *Appl. Surf. Sci.*, **428**: 17 (2018).
41. B. Starman, H. Hallberg, M. Wallin, M. Ristinmaa, and M. Halilovic, *Int. J. Mech. Sci.*, **176**: 105535 (2020).
42. H. Soyama, *J. Mater. Proc. Technol.*, **269**: 65 (2019).
43. H. Soyama, *Metals*, **10**: 63 (2019).
44. H. Soyama, C. R. Chighizola, and M. R. Hill, *J. Mater. Process. Tech.*, **288**: 116877 (2020).
45. B. N. Mordyuk, G. I. Prokopenko, M. A. Vasylyev, and M. O. Iefimov, *Mater. Sci. Eng. A*, **458**: 253 (2007).